J. Membrane Biol. 130, 149–162 (1992)

The Journal of
Membrane Biology

A TEA-Insensitive Flickering Potassium Channel Active around the Resting Potential in Myelinated Nerve

Duk-Su Koh, Peter Jonas†, Michael E. Bräu, and Werner Vogel
Physiologisches Institut, Justus-Liebig-Universität, W-6300 Giessen, Germany, and †Max-Planck-Institut für Medizinische Forschung, Abteilung Zellphysiologie, W-6900 Heidelberg, Germany

Summary. A novel potassium-selective channel which is active at membrane potentials between −100 mV and +40 mV has been identified in peripheral myelinated axons of *Xenopus laevis* using the patch-clamp technique. At negative potentials with 105 mM-K on both sides of the membrane, the channel at 1 kHz resolution showed a series of brief openings and closings interrupted by longer closings, resulting in a flickery bursting activity. Measurements with resolution up to 10 kHz revealed a single-channel conductance of 49 pS with 105 mM-K and 17 pS with 2.5 mM-K on the outer side of the membrane. The channel was selective for K ions over Na ions (P_{Na}/P_K = 0.033). The probability of being within a burst in outside-out patches varied from patch to patch (>0.2, but often >0.9), and was independent of membrane potential. Open-time histograms were satisfactorily described with a single exponential (τ_o = 0.09 msec), closed times with the sum of three exponentials (τ_c = 0.13, 5.9, and 36.6 msec). Sensitivity to external tetraethylammonium was comparatively low (IC_{50} = 19.0 mM). External Cs ions reduced the apparent unitary conductance for inward currents at E_m = −90 mV (IC_{50} = 1.1 mM). Ba and, more potently, Zn ions lowered not only the apparent single-channel conductance but also open probability. The local anesthetic bupivacaine with high potency reduced probability of being within a burst (IC_{50} = 165 nM). The flickering K channel is clearly different from the other five types of K channels identified so far in the same preparation. We suggest that this channel may form the molecular basis of the resting potential in vertebrate myelinated axons.

Key Words patch clamp · myelinated nerve fiber · potassium channel · flicker kinetics · resting potential

Introduction

In contrast to the well-described changes of membrane conductances during an action potential, little is known about generation of the resting potential in neurons. In these cells, the resting potential is about −70 mV and is, thus, likely to be caused by a potassium selective conductance (Hille, 1992). This conductance seems to be distinct from the delayed rectifier K channels with regard to pharmacological and electrophysiological properties. A potential-independent ("leakage") K conductance which cannot be blocked by the classical K channel blocker tetraethylammonium (TEA) has been suggested to be responsible for the resting potential in sympathetic ganglia (Jones, 1989), invertebrate axons (Chang, 1986), and vertebrate myelinated axons (Schmidt & Stämpfli, 1966).

In vertebrate myelinated nerve fibers, the situation is puzzling because of the electrically and pharmacokinetically complicated organization of the fiber around the node. Paranodal and internodal K channels probably contribute to the resting potential (Chiu & Ritchie, 1984; Baker et al., 1987) because of the low resistance of the axoglial junction (Barrett & Barrett, 1982). Moreover, most of the leakage current has been suggested to flow through the periaxonal space (Baker et al., 1987) rather than through the nodal membrane. Therefore, attempts to study the ionic basis of the resting potential and leakage current led to the conclusion that all ions contribute to the leakage conductance, but none of them contributes to the resting potential (Jack, 1976; Baker et al., 1987). Obviously, methods other than the classical voltage-clamp experiments (Nonner, 1969) are necessary to approach this problem.

Patch-clamp techniques on amphibian myelinated nerve fibers have been a useful tool to identify, on the single channel level, three different delayed rectifier K channels (I, F, S channels; Jonas et al., 1989) and two K channels which are controlled by intracellular ATP and by internal Ca ions (Jonas et al., 1991). All these channels except the S channel may have a low open probability around the resting potential under physiological conditions. Moreover, all are blocked by less than 10 mM external TEA. Therefore, these channels are not likely to provide a major contribution to the axonal resting po-

tential which is almost TEA-resistant (Schmidt & Stämpfli, 1966).

We have now identified a potassium-selective channel with weak potential dependence by performing patch-clamp experiments on myelinated nerve fibers. This channel is fairly insensitive to external TEA, but is blocked by external Ba, Cs, and Zn ions and by the local anesthetic bupivacaine. For the first time, direct evidence is given for a K specific axonal leakage channel setting the resting potential which has been postulated for many years (Hille, 1973, 1992). Some of the results have been presented to the German Physiological Society (Koh et al., 1991).

Materials and Methods

Preparation and Patch-Clamp Technique

The method of Hamill et al. (1981) was applied to myelinated nerve fibers as described previously (Jonas et al., 1989, 1991). Briefly, the tibial and peroneal nerves of the clawed toad (*Xenopus laevis*) were dissected and desheathed. The fibers were incubated in Ringer solution containing 3–3.5 mg/ml of collagenase (Worthington type CLS II, Biochrom, Berlin, Germany) for 135 min and subsequently treated with 1 mg/ml of protease (type XXIV, Sigma, St. Louis, MO) for 35 min in Ca-free Ringer solution. During incubation, the temperature was kept constant at 23.5 ± 0.3°C and mild shaking was applied. The nerve was cut into 3–4 mm long segments, gently stirred to dissociate nerve fibers, and transferred to 35 mm cell culture dishes (Falcon, Becton Dickinson, NJ), with the bottom coated with laboratory grease (Glisseal, Borer Chemie, Solothurn, Switzerland) to improve the attachment of the fibers. The pipettes were pulled from borosilicate glass tubes (GC150, Clark Electromedical Instruments, Pangbourne, England), coated fairly close to the tip with Sylgard 184 (Dow Corning, Seneffe, Belgium), and heat-polished directly before the experiment. Pipettes with 40 ± 5 MΩ resistance were used, except in Fig. 11. Most of the experiments were performed in the outside-out configuration. Currents were measured using an EPC-7 patch clamp amplifier (List, Darmstadt, Germany), filtered with its internal 10 kHz filter, and stored on video tape via a modified PCM-501ES pulse code modulation unit (Sony, Japan). The PCM unit itself did not cause any significant attenuation of signals up to 10 kHz. For analysis, data were replayed from tape, filtered with a 4-pole low-pass Bessel filter (−3 dB frequency either 1 or 10 kHz), and digitized with a Labmaster TM-40 AD/DA board (Scientific Solutions, Solon, OH). The sampling frequency was twice or four times the corner frequency of the low-pass filter, except in Fig. 5.

All recordings were made at 14 ± 2°C. Errors are given as standard errors of the mean (SEM) unless otherwise noted. Membrane potentials (E) are given for the inner side with respect to the outer side of the membrane, inward currents are illustrated as downward deflections, and closed states are marked by the letter C and an arrow-head (▶).

Solutions

Ringer solution contained (in mM): 110 NaCl, 2.5 KCl, 2 $CaCl_2$, and 5 BES (N,N-bis(2-hydroxyethyl)-2-aminoethanesulphonic acid), pH 7.4. 105 mM-K_o, external solution, contained: 105 KCl, 13 NaCl, 2 $CaCl_2$, and 5 BES, pH 7.4. Potential-dependent Na channels were blocked by adding 100 nM tetrodotoxin to the external solutions. 105 mM-K_i, internal solution, contained: 105 KCl, 13 NaCl, 5 BES, 3 EGTA (ethylenebis(oxyethylenenitrilo)-tetraacetate), pH 7.2. Tris (tris(hydroxymethyl)aminomethane) base was used to adjust the pH. In some experiments, blockers were applied to the bath by adding small amounts of concentrated stock solution and mixing the solutions subsequently. In most of the experiments, drugs were applied rapidly with a multibarrel perfusion system. TEACl (tetraethylammonium chloride), $BaCl_2$, and $ZnCl_2$ were from Merck (Darmstadt, Germany), CsCl and bupivacaine were from Sigma (St. Louis, MO). Stock solutions (500 mM) of inorganic blockers were prepared in 105 mM-K_o, stock solution (10 mM) of bupivacaine was prepared in distilled water.

Analysis of Single-Channel Currents

At 1 kHz filter frequency (*see* Fig. 2*B* and *E*), the gating of the flicker channel at $E_m < -40$ mV was so rapid that the full open and closed levels were not resolved. This made the estimation of the single-channel amplitude and the kinetic parameters ambiguous. Therefore, these measurements at negative potentials were restricted to patches with an extraordinarily low background noise allowing recording at 10 kHz resolution (*see* Fig. 2*A* and *D*). Apparent unitary current amplitudes, i, at $E_m \leq -30$ mV were determined from point amplitude histograms, which at this high resolution showed two distinct peaks (*see* Fig. 2*C* and *F*). In 105 mM-K_o at potentials $E_m \geq -40$ mV or in Ringer solution in the whole investigated potential range, flickering was less pronounced, and therefore amplitude measurements were performed on a digital storage oscilloscope (NIC-310, Nicolet, Madison, WI) at 1 kHz resolution. At $E_m = -30$ and -40 mV, the two methods gave identical results.

The mean current during bursts, $I_{\text{mean-burst}}$, and the mean current during the total recording, $I_{\text{mean-total}}$, were calculated as the mean value from the respective sample points. The measurement of these parameters did not require high resolution recording and was therefore used in all pharmacological experiments (*see* Figs. 7–10, Table).

Open probability during bursts (*see* Fig. 4) was obtained from $I_{\text{mean-burst}}$ divided by the unitary current amplitude. Probability of being within a burst was estimated as $I_{\text{mean-total}}$ divided by $I_{\text{mean-burst}}$.

Open and closed time histograms were obtained at 10 kHz resolution after idealization. A semiautomatic procedure was used to detect channel events. The threshold was set to 50% of the single-channel current. Only patches with one active channel were analyzed. The close time histograms showed distinct exponential components with mean time constants of 0.13 msec, 5.9 msec, and 36.6 msec (*see* Fig. 6). Rather arbitrarily, bursts were defined as any series of openings separated by gaps that were less than 1.0 msec (*see* Colquhoun & Hawkes, 1982). This value was chosen because it separated well the first and second component and because closings of this length could be reliably detected even at 1 kHz resolution. The logarithm of the frequency density was fitted with exponential functions using unweighted nonlinear least-squares fit (modified Gauss-Newton method). Stationary fluctuation analysis was performed with a fast Fourier transformation algorithm yielding the single-sided spectral density function (*see* DeFelice, 1981). The spectrum from recordings with no chan-

nel opening was subtracted. The obtained difference spectrum was corrected for the frequency response of the total recording system, which was determined with white noise from a 12 MΩ resistor connected to the headstage of the EPC-7. Spectral density data were fitted with a Lorentzian function

$$S(f) = S(0)/[1 + (f/f_c)^2],$$

where S denotes the spectral density, f the frequency, and f_c the corner frequency.

Results

With 40 MΩ pipettes corresponding to a patch area of <1 μm^2 (Sakmann & Neher, 1983), flicker channels were found in about 80% of patches obtained from thin fibers (≤ 5 μm in myelin diameter) and in about 20% of patches from thicker fibers (>5 μm). The highest and the average number of simultaneously open flicker channels were eleven and two in such patches, respectively. No difference of channel density in nodal, paranodal, and internodal regions of the axon was observed. Like other K channels, flicker channels could more easily be investigated with a high potassium concentration on both sides of the membrane (Jonas et al., 1989). Many experiments were performed at negative membrane potential ($E_m = -90$ mV) to avoid superposition with other types of voltage-dependent K channels. Results were obtained from 88 membrane patches, 32 of which were analyzed in detail.

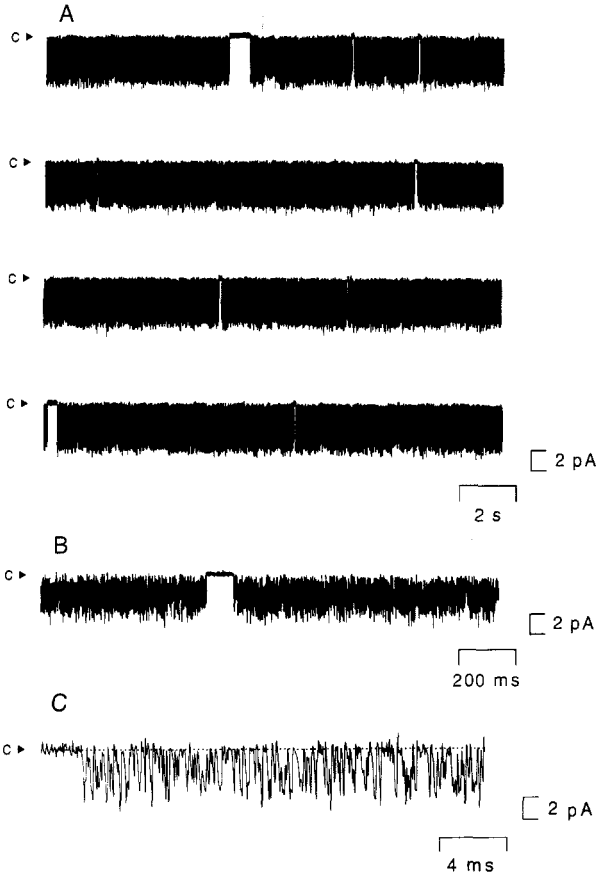

Fig. 1. Typical activity of the flicker channel at different time scales and different resolutions. Outside-out patch. Bath: 105 mM-K_o, pipette: 105 mM-K_i. Membrane potential $E_m = -90$ mV, filter frequency: 1 kHz (*A*, *B*) and 10 kHz (*C*).

Electrophysiological Properties

The activity of a single flicker channel is shown in Fig. 1 at different time scales. At negative membrane potential ($E_m = -90$ mV) and with symmetrical potassium concentration on both sides of the membrane (105 mM-K_o/105 mM-K_i), the channel showed a series of brief openings and closings interrupted by longer closings, resulting in a flickery, bursting appearance at 1 kHz resolution. The rapid openings and closings within bursts are not completely resolved at 1 kHz (Fig. 1*B*). Even at a resolution of 10 kHz, many events were too short to be clearly detectable (Fig. 1*C*).

Flickering is the dominating feature of the gating of the channel at potentials $E_m < -40$ mV (Fig. 2*A* and *B*). Measurements with 10 kHz resolution revealed that the rapid transitions within bursts in fact occur between the fully open and fully closed state, appearing as high density of sample points at the two current levels. Thus, the single-channel current can be reliably estimated from the peaks of the corresponding point-amplitude histograms as shown in Fig. 2*C*. In contrast, the current traces at 1 kHz resolution (Fig. 2*B*) do not show the "real" open channel level, but rather a mean value of the current during bursts.

At potentials $E_m \geq -40$ mV (Fig. 2*D*), the channel is almost entirely in the open state during bursts with a few rapid transitions to the closed state. In accordance with this observation, amplitude histograms constructed from recordings filtered at 10 kHz (Fig. 2*F*) and current measurements at 1 kHz (Fig. 2*E*) gave identical values of single-channel current at these potentials.

Single-channel conductance properties and ion selectivity of the flicker channel were investigated in the experiments shown in Fig. 3. Recordings with 105 mM-K_o and with Ringer solution on the outer side of the membrane at different potentials are shown in Fig. 3*A* and *B*, respectively. In accordance with the results of Fig. 2, the flickering within bursts is particularly apparent in 105 mM-K_o at negative

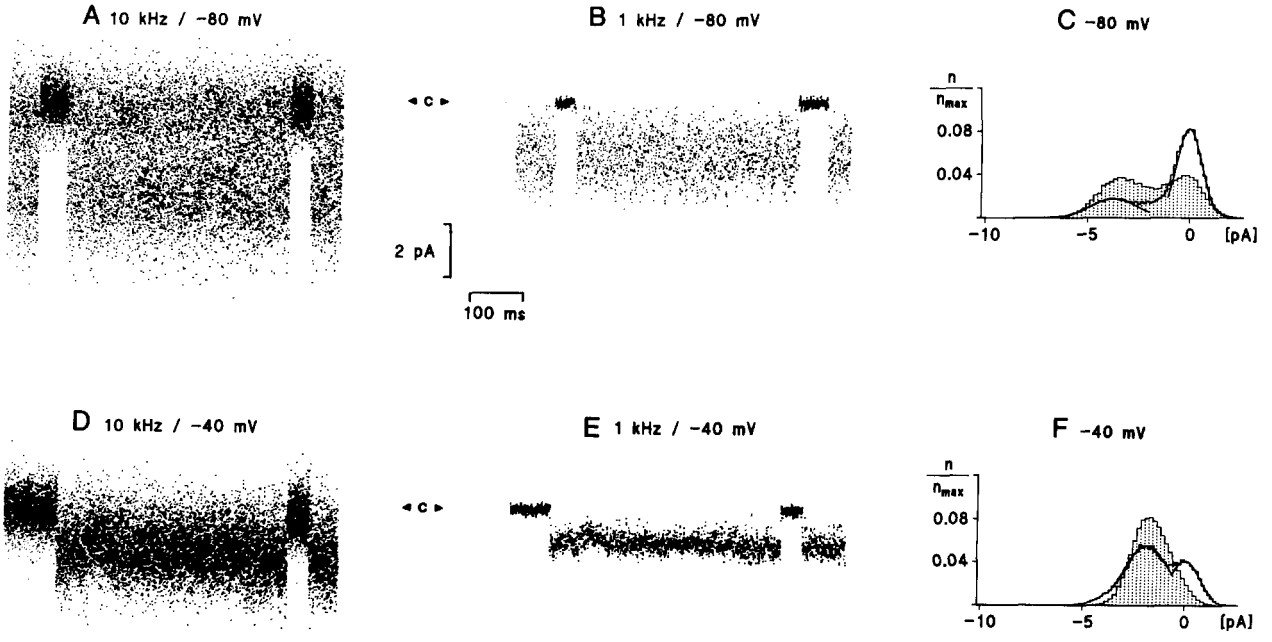

Fig. 2. Fast gating of the flicker channel recorded at different potentials and at different resolutions. Membrane potentials (E_m) were −80 mV (*A*, *B*), and −40 mV (*D*, *E*). Filter frequencies were 10 kHz (*A*, *D*) and 1 kHz (*B*, *E*), and corresponding sample frequencies were 20 kHz and 4 kHz, respectively. Outside-out patch. Bath: 105 mM-K_o, pipette: 105 mM-K_i. Note the changes in current distribution after filtering at lower cut-off frequency. (*C*, *F*) Histograms of data points at $E_m = -80$ mV (*C*) and $E_m = -40$ mV (*F*) filtered at 10 kHz. Data were obtained either from 6.4 sec total recordings (clear) including the traces in (*A*) and (*D*) or from recordings excluding the gaps between bursts (shaded). Histograms were fitted with two Gaussian curves which represent open and closed states. The amplitude of the single-channel current was determined as the difference between the peaks.

potentials. Flickering was not observed in Ringer solution at membrane potentials between −120 and 40 mV, even when the frequency resolution was increased to 10 kHz.

The single-channel current voltage relations (*i-E*) with 105 mM-K_o and with Ringer solution are shown in Fig. 3*C*. The single-channel current was obtained with the histogram method at 10 kHz for $E_m \leq -30$ mV in 105 mM-K_o. For $E_m \geq -40$ mV in 105 mM-K_o and at all potentials in Ringer solution, a manual measurement at 1 kHz was performed. The *i-E* curve for 105 mM-K_o shows a slight inward rectification. The mean single channel conductance is 49 pS. The *i-E* curve for Ringer solution on the outer side of the membrane shows a single-channel conductance of 17 pS for outward currents. The reversal potential obtained by polynomial interpolation was $E_{rev} = -70$ mV. The permeability of the flicker channel for Na ions as compared to K ions can thus be calculated using the Goldman equation (*see* Hille, 1992) as $P_{Na}/P_K = 0.033$ indicating that the channel is fairly selective for K ions over Na ions.

In addition to the single channel *i-E*, we evaluated the *I-E* for the total mean current to predict the macroscopic currents generated by the channel. The *I-E* relation for the total mean current with 105 mM-K_o is shown in Fig. 4*A* (filled symbols). In contrast to the single-channel *i-E*, the total mean current does not increase at potentials $E_m < -60$ mV, which is due to the voltage dependence of the rapid gating process. The mean current during bursts (Fig. 4*A*, open symbols) is, as expected, higher than the total mean current at all membrane potentials.

From the total mean current and the mean current during bursts, probability of being within a burst could be calculated (*see* Materials and Methods). Figure 4*B* shows that the probability of being within a burst was independent of membrane potential. For excised patches, this probability varied between 0.2 and 0.95 in different experiments. In cell-attached patches, bursting activity was lower than in excised patches. This may reflect the modulation of the channel activity by cytoplasmic factors.

Open probability during bursts (Fig. 4*C*) has been obtained as the ratio of mean current during bursts and corresponding single-channel current (Fig. 3*C*; *see* Materials and Methods). In contrast to the probability of being within a burst, it decreases at potentials less than −40 mV. The major reason

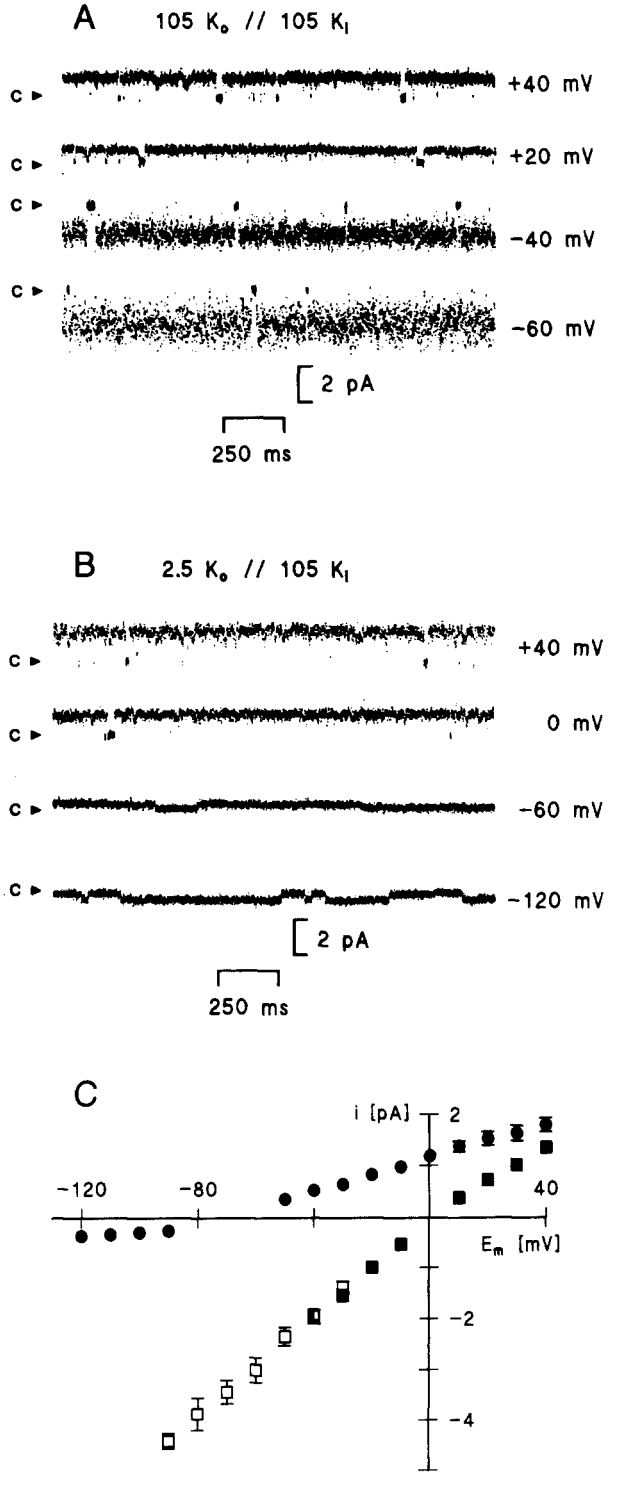

Fig. 3. Single-channel conductance properties and ion selectivity. Original traces with 105 mM-K_o (*A*) or with Ringer solution (*B*) as external solutions at different membrane potentials. Outside-out patch with 105 mM-K_i as internal solution, filter frequency 1 kHz. (*C*) Current-voltage relations of single-channel currents in Ringer solution (circles, 3 patches) and in 105 mM-K_o (squares, 3 patches). Data in symmetrical 105 mM-K measured from a storage oscilloscope (filter 1 kHz) for potentials $E_m \geq -40$ and determined with the histogram method for potentials $E_m \leq -30$ mV. Data in Ringer solution measured from oscilloscope. Note slight inward rectification in 105 mM-K_o. Error bars smaller than symbol size are omitted.

for the deflection of the total mean current-voltage relation (Fig. 4*A*) is thus the decrease of open probability during bursts at more negative potentials.

Although the probability of being within a burst studied under stationary conditions (Fig. 4*B*) gave no evidence that the flicker channel shows properties of time-dependent inward rectification (Baker et al., 1987), we also tested its behavior under nonstationary conditions during a voltage jump from $E_m = -40$ mV to $E_m = -120$ mV using an axon-attached patch which displayed low probability of being within a burst (Fig. 5). As can be seen in 5 representative recordings and in the averaged current trace from 56 recordings, bursting activity occurred randomly with minor pulse-associated changes. This is in contrast to inward rectifier behavior (*e.g.*, Takahashi, 1990).

Channel gating was investigated by constructing open and closed time histograms at negative membrane potentials ($E_m = -90$ mV or -100 mV) with 10 kHz resolution. The frequency density was plotted against time on a semi-logarithmic scale to visualize slow components. An example of an open time histogram is shown in Fig. 6*A*. The data were satisfactorily described by a single exponential function with $\tau_o = 0.092 \pm 0.007$ msec (five patches at $E_m = -90$ mV, one patch at -100 mV). The corresponding closed time histogram is shown in Fig. 6*B*. For closed times < 1 msec, the data can be fitted by an exponential with $\tau_{c,1} = 0.125 \pm 0.013$ msec. For closed times < 150 msec (Fig. 6*C*), two additional components were apparent with time constants $\tau_{c,2} = 5.9 \pm 1.2$ msec, $\tau_{c,3} = 36.6 \pm 3.3$ msec (two patches at $E_m = -90$ mV, one patch at $E_m = -100$ mV). Occasionally, the channel remains in the closed state for several seconds.

From the time constants of the histograms the corner frequency of flickering could be estimated as $f_c = 1/2\pi \times (1/\tau_o + 1/\tau_{c,1}) = 3.0$ kHz. It should be noted, however, that the false event rate at 10 kHz resolution is $0.2 - 0.4\ s^{-1}$ under our recording conditions (Colquhoun & Sigworth, 1983, p. 204), and moreover, events shorter than the dead time $T_d = 0.018$ msec could not be detected (*see also* Colquhoun & Sigworth, 1983, p. 216).

As some of the fast events may have been missed even at 10 kHz resolution, we investigated the fast gating process using stationary fluctuation analysis. The spectral density function corrected for frequency response of the recording system as

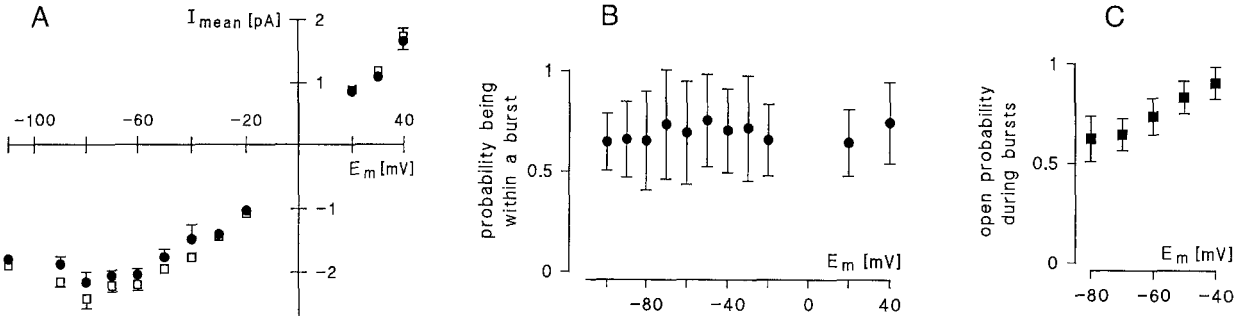

Fig. 4. Potential dependence of bursting activity under stationary conditions. (*A*) Current-voltage relations of mean currents measured from total recordings which lasted 6.4–12.8 sec ($I_{\text{mean-total}}$, filled symbols) and measured during bursts only ($I_{\text{mean-burst}}$, open symbols). Data from three outside-out patches and one inside-out patches, symmetrical 105 mM-K. (*B*) Probability of being within a burst determined as mean current during bursts divided by total mean current. Error bar indicates standard deviations (SD). (*C*) Open probability during bursts determined as mean current during bursts divided by unitary current amplitude (*see* Fig. 3*C*; Materials and Methods).

shown in Fig. 6*D* was sufficiently described by a single Lorentzian component with $f_c = 4.6 \pm 0.2$ kHz (four patches at $E_m = -90$ mV). The f_c value from the spectral density function is slightly higher than the f_c estimated from the τ_o and $\tau_{c,1}$ values (see above). This may be due to brief events missed during the idealization procedure.

To study the nature of the rapid flickering, we further investigated if it was caused by one of the ions in our solutions. A flickery block of other ion channels by various different ions (Na, Cs, HEPES) has been reported previously (Yellen, 1984; Yamamoto & Suzuki, 1987; Quayle, Standen & Stanfield, 1988). In contrast, rapid gating of the flicker channel was also observed when Tris, Na, and Ca ions were omitted from the outer solution and Tris, Na, and EGTA ions were omitted from the inner solution. Moreover, replacement of BES by HEPES and variation of pH (5.7 – 9.3) on both sides of the membrane had no obvious effects on this fast process. We therefore suggest that the fast flickering might result either from the interaction between K ions and the channel or from an intrinsic fast gating mechanism of the channel protein.

In conclusion, the flicker channel is a potassium selective, weakly potential-dependent channel with complex kinetic properties. The time course of its gating ranges over orders of magnitude between 100 μsec and several seconds.

Pharmacological Properties

In order to characterize pharmacological properties of the flicker channel which may distinguish it from other K channels, we first tried classical blockers of K channels like TEA, Cs, and Ba, but also searched for potent and specific inhibitors.

The effect of external TEA at negative membrane potential is illustrated in Fig. 7. Very high concentrations of TEA (50 mM) reduce the mean current during bursts without noticeably changing the channel activity (Fig. 7*A*, Table). The block of the current during bursts is not significantly different from the block of the total mean current. Thus, TEA reduces only the apparent single-channel current but does not change the probability of being within a burst. The blocking kinetics of TEA appear to be fast as reported for other axonal K channels (Jonas et al., 1991). In Fig. 7*B* the fractional block of the mean current during bursts was plotted against TEA concentration. The data points can be satisfactorily described by a Hill coefficient of one and a 50%-inhibitory concentration $IC_{50} = 19.0$ mM. Compared to other K channels in this preparation, the flicker channel is very insensitive to this blocker.

In contrast, at negative membrane potentials the flicker channel is fairly sensitive to external Cs ions as shown in Fig. 8*A*. At $E_m = -90$ mV, Cs reversibly reduces the mean current during bursts with fast blocking kinetics but does not change the probability of being within a burst (Fig. 8*A*, Table). The mean current during burst *vs.* voltage plot in Fig. 8*B* shows that the Cs block is highly potential dependent, being less pronounced at positive than at negative potentials. Voltage-dependent block by Cs ions is a common feature of many K channels. The voltage dependence can be quantitatively described with the function

$$i_{Cs}/i_{control} = [1 + ([Cs]/K_d(E_m))]^{-1}$$
$$\text{with } K_d(E_m) = K_d(0) \exp(z'EF/RT)$$

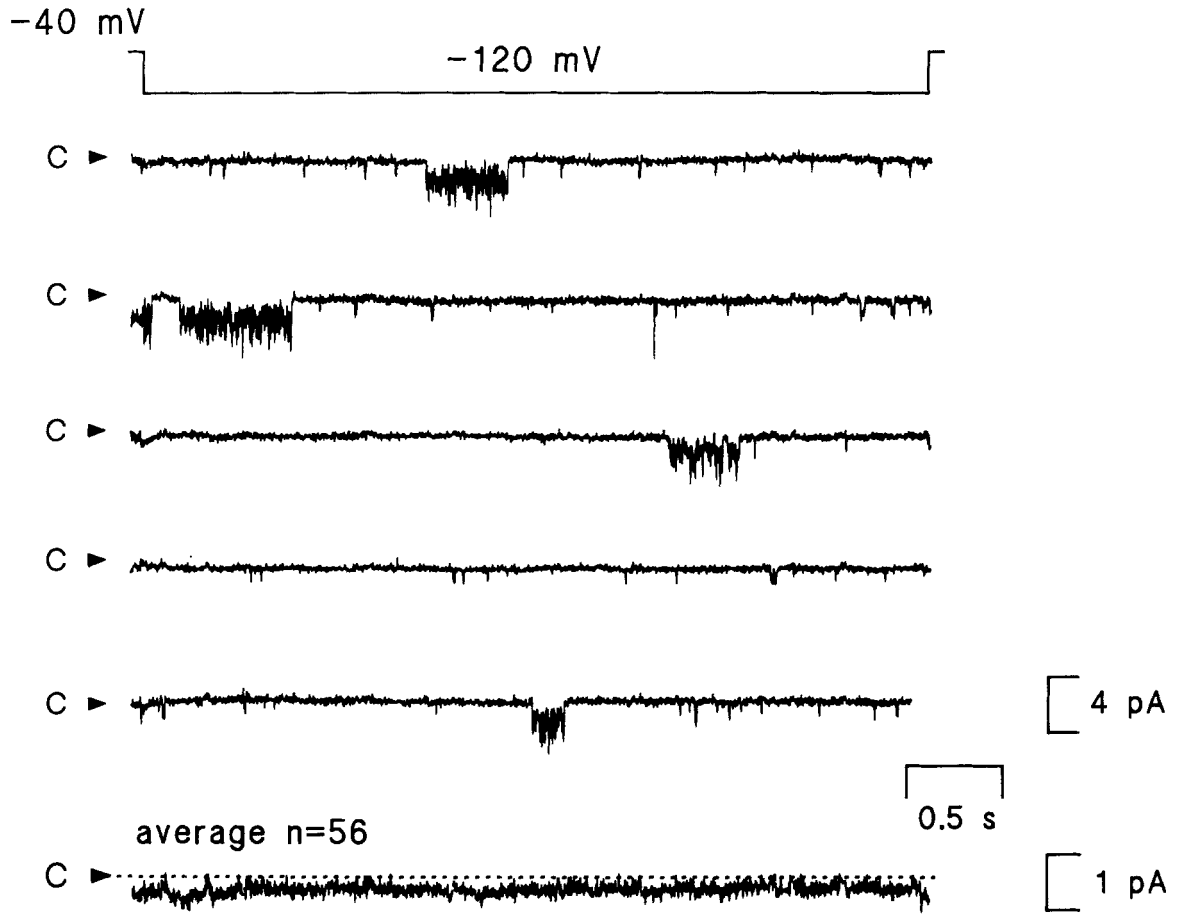

Fig. 5. Potential dependence of bursting activity under non-stationary conditions. Upper five recordings show voltage-jumps from $E_m = -40$ mV to $E_m = -120$ mV lasting 4 sec applied to an axon-attached patch with low channel activity. Bath: 105 mM-K_i, pipette: 105 mM-K_o. Lowest trace shows average of 56 recordings. Capacitative and leakage currents were subtracted digitally using empty recordings. Zero current level is indicated by the dashed horizontal line. Filter frequency 1 kHz, sample frequency 0.5 kHz.

(see Quayle et al., 1988; Grygorezyk & Schwarz, 1985), where $i_{Cs}/i_{control}$ is the measured current as a fraction of control value, [Cs] is the concentration of Cs ions, K_d is the dissociation constant, and z' is the product of the valency z of the blocking ion and the fraction of the transmembrane potential sensed during its movement into the channel. Analysis of the *I-E* curves in control and with 2.1 mM Cs in the potential range of -80 to -20 mV reveals a $K_d(0)$ of 112 mM and a z' of 1.59 (*see* Quayle et al., 1988). The z' value greater than one may indicate that the flicker channel is a multi-ion channel (*see* Hille & Schwarz, 1978). Further evidence in favor of this assumption may be obtained from the plot of fractional block of the mean current during bursts against Cs concentration at $E_m = -90$ mV shown in Fig. 8*C*, yielding an $IC_{50} = 1.1$ mM and a Hill coefficient of 1.79.

The block by external Ba ions at $E_m = -90$ mV is shown in Fig. 9*A*. The original traces already demonstrate that 2 mM and 20 mM Ba, unlike Cs, reduce the mean current during bursts as well as the burst length and accordingly increase the number of longer closings. The reduction of probability of being within a burst is quantified in the Table, which shows that the block of the total mean current for 20 mM Ba is significantly stronger than the block of the mean current during bursts. The voltage dependence of the block is demonstrated in the *I-E* relations for the total mean current given in Fig. 9*B*. As with the block by Cs, the block by Ba ions is more pronounced at negative potentials.

The effect of Zn on the flicker channel was investigated because fluxes of K ions in skeletal muscle were sensitive to both Ba and Zn (Spalding, Swift & Horowicz, 1986). Zn ions in a concentration range

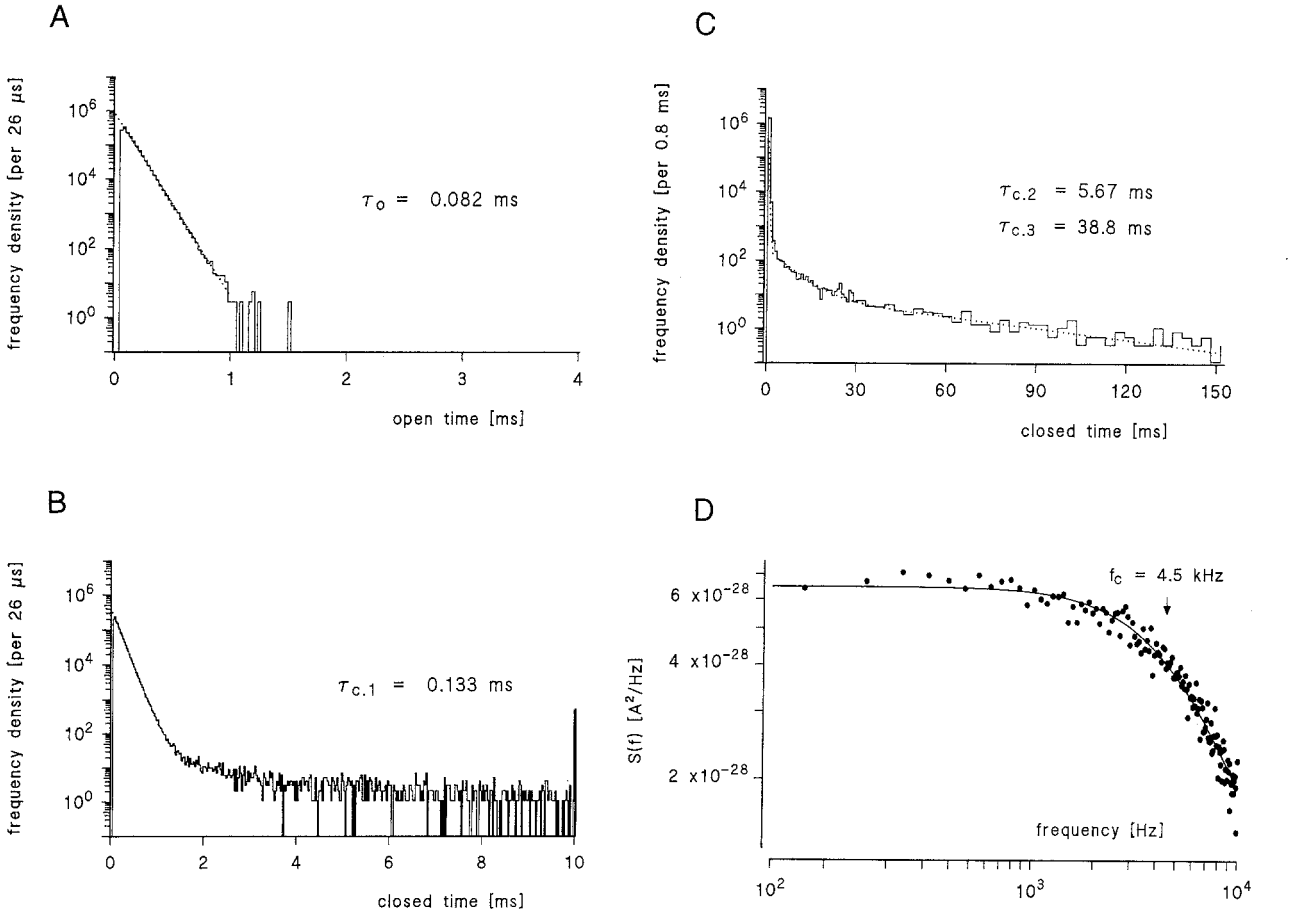

Fig. 6. Kinetics of the flicker channel. (*A*) (*B*) (*C*) Open and closed time histograms at $E_m = -100$ mV. Logarithm of frequency density plotted *vs.* time. Outside-out patch, bath: 105 mM-K_o, pipette: 105 mM-K_i. Current traces were filtered at 10 kHz and sampled with 38.5 kHz. Total number of events 1.452×10^6, total length of analyzed record 500 sec. (*A*) Open time histogram 0–10 msec fitted with a single exponential, $\tau_o = 0.082$ msec. (*B*) Closed time histogram 0–10 msec. Data between 0 and 1 msec were fitted with a single exponential, $\tau_{c.1} = 0.133$ msec. All events beyond 10 msec are summed up at the end of the histogram. (*C*) Closed time histogram 0–150 msec fitted with three exponential components, $\tau_{c.2} = 5.67$ msec, $\tau_{c.3} = 38.8$ msec, $\tau_{c.1}$ constrained to same value as in (*B*). Fits were based on the logarithmic data. (*D*) Stationary fluctuation analysis from another outside-out patch at $E_m = -90$ mV. Gaps between bursts included, total length of analyzed record 9.6 sec. Curve is drawn according to a Lorentzian function with $f_c = 4.5$ kHz as obtained by least-squares fit.

0.2 mM – 2 mM blocked the channel in a similar way to Ba, reducing the mean current during bursts as well as the burst length (Fig. 9*C* and Table). As compared to Ba, Zn ions blocked much more effectively, had a stronger effect on probability of being within a burst than on mean current during bursts, and induced longer closings between bursts. In contrast to Cs and Ba, Zn ions reduced outward currents and inward currents to a similar extent (Fig. 9*D*).

The potency of all the blockers investigated so far was rather low. Effects of anesthetics on the resting membrane conductance in squid axon have been reported (Haydon, Requena & Simon, 1988). We tried bupivacaine, an uncharged local anesthetic. Fig. 10 shows that bupivacaine applied to the outer side of the membrane hardly affected the single-channel conductance, but it reversibly reduced probability of being within a burst by causing long closings similar to Zn ions. The plot of fractional block against bupivacaine concentration shown in Fig. 10*B* demonstrates that bupivacaine is the most potent blocker with an IC_{50} value of 0.165 μM.

Addressing the question of the functional role of the flicker channel was impeded by two facts. Firstly, it was not possible to establish the whole-cell configuration with our nerve fiber preparation, and secondly, the effects of some of the blockers were voltage dependent (see above), making the interpretation of current-clamp measurements ambiguous. We therefore recorded ionic currents from "macropatches" containing several channels under voltage-clamp conditions in the range of possible

Table. Fractional block of total mean current and mean current during bursts

Test solution (mM)	Total block (mean ± SEM)	Block during bursts (mean ± SEM)	Significant difference
5 TEA	0.342 ± 0.047	0.222 ± 0.012	no
50 TEA	0.731 ± 0.014	0.728 ± 0.011	no
0.2 Cs	0.217 ± 0.014	0.211 ± 0.088	no
2 Cs	0.656 ± 0.050	0.686 ± 0.022	no
2 Ba	0.561 ± 0.034	0.384 ± 0.018	no
20 Ba	0.902 ± 0.009	0.660 ± 0.092	yes
0.2 Zn	0.677 ± 0.030	0.262 ± 0.039	yes
2 Zn	0.961 ± 0.019	0.637 ± 0.013	yes

Mean currents were measured either from total recordings (6 to 30 sec) including closures or during bursts only, and related to mean currents in control at $E_m = -90$ mV. Three outside-out patches for each concentration. Significance tested with two-sided t test, $\alpha = 0.05$.

resting membrane potentials. At $E_m = -90$ mV, an inward current with 105 mM-K_o was observed (Fig. 11), which at higher time resolution shows the rapid kinetics typical for the flicker channel (*not shown*). It could not be blocked by 10 mM TEA, but was inhibited by Ba and Cs ions. Its pharmacological features were thus similar to those of the flicker channel. Therefore, the flicker channel appears to be the dominant channel at this membrane potential. At $E_m = -60$ mV, a larger fraction of inward current is blocked by TEA and may thus be mediated by voltage-dependent delayed-rectifier K channels (*e.g.*, I channels, Jonas et al., 1989). The weaker effects of Cs and Ba ions at this potential probably reflect the voltage dependence of block as shown in Figs. 8 and 9. We thus conclude that the flicker channel, at least under some conditions, can contribute to the resting conductances of vertebrate axons.

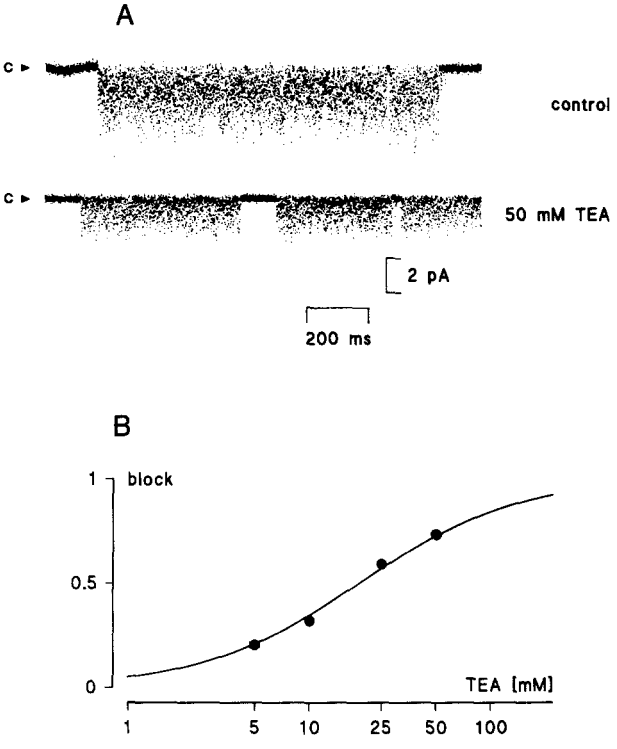

Fig. 7. TEA block. (*A*) Recordings with 105 mM-K_o (control) and with 105 mM-K_o containing 50 mM external TEA in the bath, outside-out patch, pipette: 105 mM-K_i, $E_m = -90$ mV. (*B*) Fractional block of mean current during bursts *vs.* concentration of TEA(c) at $E_m = -90$ mV. Data from three outside-out patches. Standard errors of the mean were smaller than symbol size. The curve represents the function $f(c) = [1 + (IC_{50}/c)^a]^{-1}$ with half-maximal inhibitory concentration $IC_{50} = 19.0$ mM and Hill coefficient $a = 1.0$ as obtained by least-squares fit.

Discussion

In this study we have identified a novel K-selective channel in myelinated nerve fibers. It is fairly insensitive to TEA, but is blocked by Cs, Ba, and Zn ions and by the local anesthetic bupivacaine.

Single Channel Properties, Kinetics, Pharmacology: A Novel Type of K Channel

The flicker channel is clearly different from the classical delayed rectifier K channels in myelinated nerve fibers and in other preparations. Only its fast gating process is voltage dependent, and the channel is hardly affected by 10 mM TEA, a concentration which almost completely blocks the delayed rectifier K channels in myelinated nerve (Jonas et al., 1989). It is also clearly distinct from the Ca-activated K

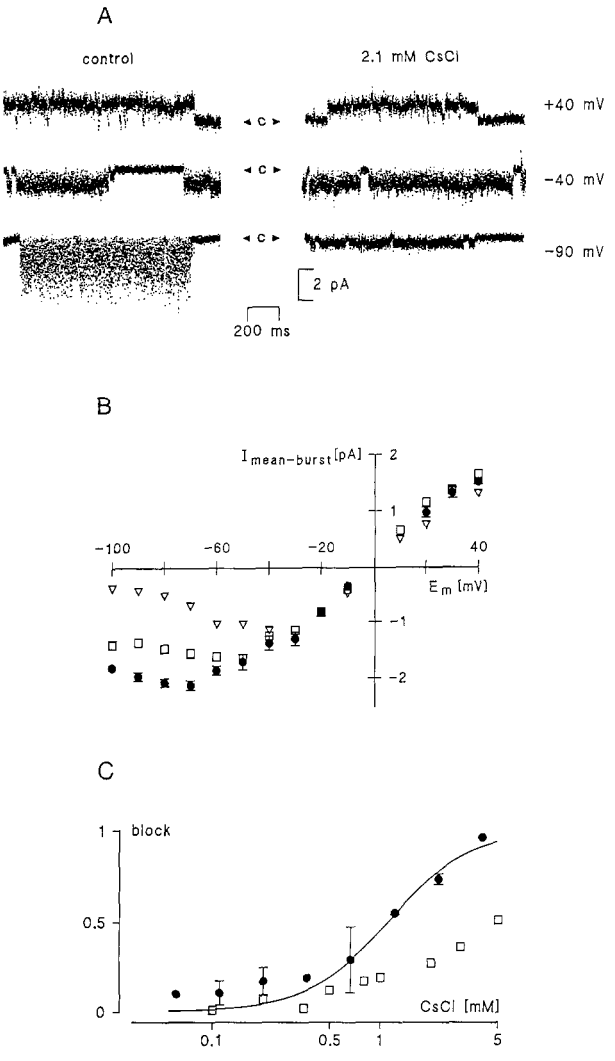

Fig. 8. Cs block. (*A*) Recordings with 105 mM-K_o and with 105 mM-K_o containing 2.1 mM CsCl in the bath at different potentials, outside-out patch, pipette: 105 mM-K_i. (*B*) Current-voltage relations of mean current during bursts ($I_{mean-burst}$) with 0.35 mM CsCl (squares) and 2.1 mM CsCl (triangles) and control (filled circles, data are pooled from four patches) in 105 mM-K_o. (*C*) Fractional block of mean current during bursts *vs.* concentration of Cs at $E_m = -40$ mV (squares) and at $E_m = -90$ mV (circles). Data from nine outside-out patches. Curve obtained as in Fig. 7*B* with $IC_{50} = 1.1$ mM and $a = 1.8$ ($E_m = -90$ mV). Data points for $c < 0.37$ mM were excluded from the fit.

channel, because it does not require Ca ions on the inner side of the membrane to be activated. The gating behavior is complex, and the fastest process shows open and closed time constants much smaller than 1 msec in high K external solution at negative membrane potentials. This flickering, which is a particularly prominent feature of the channel, does not seem to be caused by ions other than K, for example Na, Ca, or buffer ions. Therefore, it is more likely to be due to an intrinsic gating mechanism (Rae, Dewey, & Cooper, 1989). In some respects, the flickering is reminiscent of the buzz mode into which the Ca-activated K channel infrequently enters (McManus & Magleby, 1988). Rapidly flickering K channels have also been observed in red blood cells (Hamill, 1983; this channel is, however, Ca-dependent). The channel which is most similar to the axonal channel of this paper is a flickering K channel in rabbit corneal endothelium (Rae et al., 1989).

The order of potency of ion block is Zn > Cs > Ba > TEA at negative potentials. The type of block by the divalent ions (Zn, Ba) is different from that by monovalent ions (Cs, TEA). The latter reduce the apparent single channel conductance without affecting the overall bursting activity of the channel. Ba ions, and more effectively Zn ions, mainly induce several longer closings, but at higher concentrations also reduce the apparent single-channel conductance. A similar difference between the time scale of block by Cs and Ba ions has been described previously for inward rectifier K channels (Sakmann & Trube, 1984) and Ca-activated K channels (Grygorezyk & Schwarz, 1985). The Cs block is highly voltage dependent and its concentration dependence gives a Hill coefficient greater than 1, indicating that the flicker channel, similar to other types of K channels, may be a multi-ion pore (Hagiwara, Miyazaki & Rosenthal, 1976; Grygorezyk & Schwarz, 1985; Quayle et al., 1988; *see* Hille & Schwarz, 1978 for general description). The Ba block shows a voltage dependence similar to Cs, whereas the Zn block was not noticeably voltage dependent. So far, the local anesthetic bupivacaine seems to be the most potent inhibitor of this channel. It is conceivable that bupivacaine exerts its anesthetic effect on myelinated nerve fibers not only via a direct blockade of sodium channels but also via a blockade of flicker channels, successive depolarization, and inactivation of sodium channels.

Comparison with Leakage and Rectifying Conductances in Neurons

With regard to rectification and some pharmacological features, the flicker channel matches the potential-independent, TEA-insensitive "leakage" conductances demonstrated in several cells. These leakage channels are presumed to be K selective (Jones, 1989). They are blocked by Ba (Jones, 1989; Takahashi, 1990), and in some types of cells, also by Cs ions (Constanti & Galvan, 1983). In the squid axon, the leakage current is insensitive to TEA (Chang, 1986) and is blocked by general anesthetics (Haydon et al., 1988), the specific leakage conductance amounting to 0.8 mS/cm^2. In myelinated nerve, it was concluded from classical voltage-clamp experiments that the nodal membrane must have a

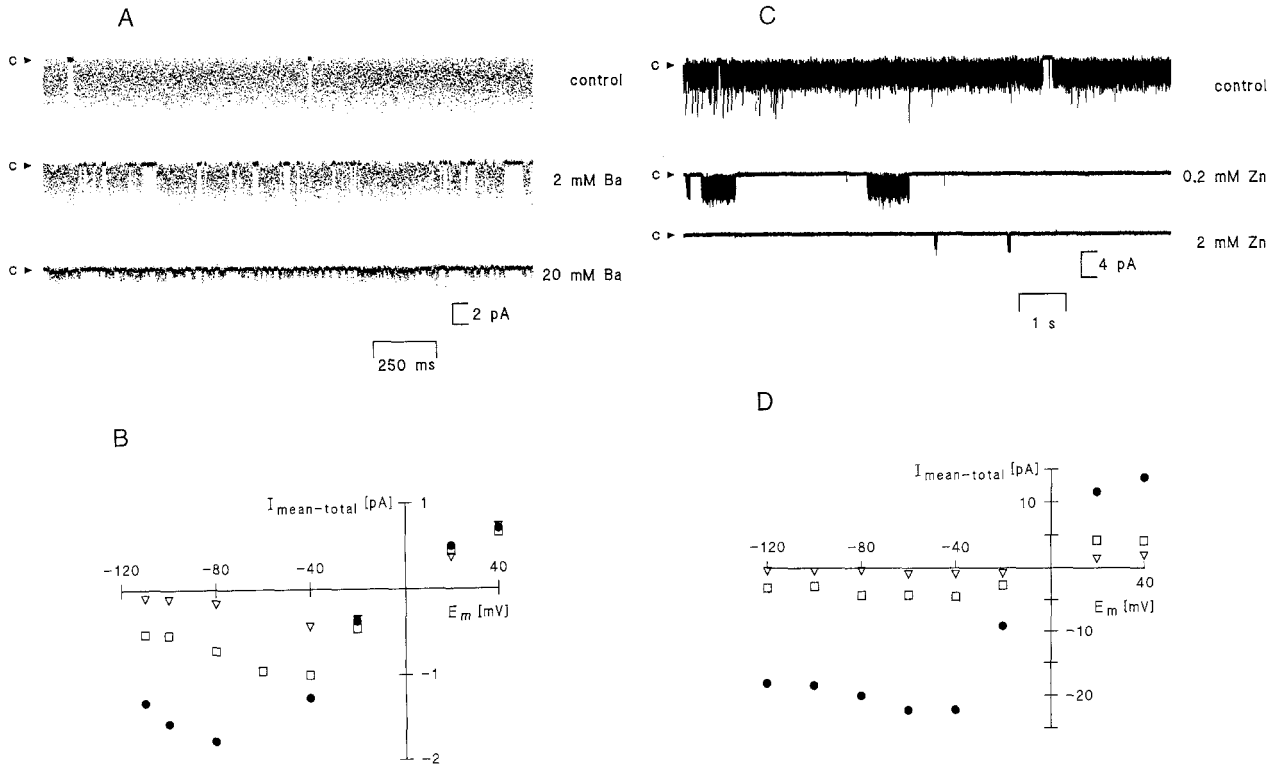

Fig. 9. Ba and Zn block. (*A*) Recordings with 105 mM-K_o (control), with 105 mM-K_o containing 2 or 20 mM $BaCl_2$ in the bath, outside-out patch, pipette: 105 mM-K_i, E_m = −90 mV. (*B*) Current-voltage relations of total mean current with 2 mM $BaCl_2$ (squares) and 20 mM $BaCl_2$ (triangles) and control (circles) in 105 mM-K_o. Data from one outside-out patch which contained two flicker channels. (*C*) Recordings in 105 mM-K_o (control), with 105 mM-K_o containing 0.2 and 2 mM $ZnCl_2$ in the bath, outside-out patch, pipette: 105 mM-K_i, E_m = −90 mV. (*D*) Current-voltage relations of total mean current with 0.2 mM $ZnCl_2$ (squares) and 2 mM $ZnCl_2$ (triangles) and control (circles) in 105 mM-K_o. Data from one outside-out patch which contained 11 flicker channels.

very high density of K-preferring, TEA-insensitive leakage channels (Hille, 1973). The specific leakage conductance estimated for the amphibian node was 40 mS/cm^2 (Hille, 1992), but most of this leak may flow through the axoglial shunt and internodal channels (Baker et al., 1987). The average flicker channel density in our experiments is two channels per patch and the single channel conductance is 17 pS in Ringer solution. Assuming an open probability of 0.5 and a patch area of 1 μm^2 (see above), the specific leakage conductance of the axonal membrane due to the flicker channel would be 0.85 mS/cm^2. This value is similar to the leakage in the internodal membrane of demyelinated vertebrate axon (less than 1 mS/cm^2, Chiu & Ritchie, 1982), suggesting that at least part of the leak may be caused by the flicker channel.

With regard to pharmacology, but not rectification, the flicker channel resembles the ubiquitous inwardly rectifying conductances in neurons. Such inwardly rectifying channels were first identified in hippocampus (Halliwell & Adams, 1982) and termed I_Q. They are insensitive to TEA, are more sensitive to block by Cs than by Ba (*e.g.*, Jones, 1989), and, at least in some types of cells, are blocked by local anesthetics (Hwa & Avoli, 1991). With regard to pharmacology, the flicker channel and I_Q are very similar. Moreover, it is noteworthy that such inwardly rectifying conductances are present in motoneurons (Takahashi, 1990) and dorsal root ganglia cells (Mayer & Westbrook, 1983), which are the somata corresponding to the axons investigated in the present paper. The presence of inwardly rectifying channels in the internodal membrane in myelinated nerve fibers was even suggested on the basis of electrotonus measurements (Baker et al., 1987). However, the flicker channel and I_Q are completely different in two important respects. Flicker channels are more selective for K ions than I_Q (*e.g.*, Takahashi, 1990), and flicker channels lack any sign of inward rectification. It thus remains unclear if there is any relation to inwardly rectifying conductances.

Physiological Role of the Channel in Myelinated Nerve Fibers

Does the flicker channel set the resting potential of the vertebrate nerve fiber? Evidence that this might be the case comes from the fact that the reversal

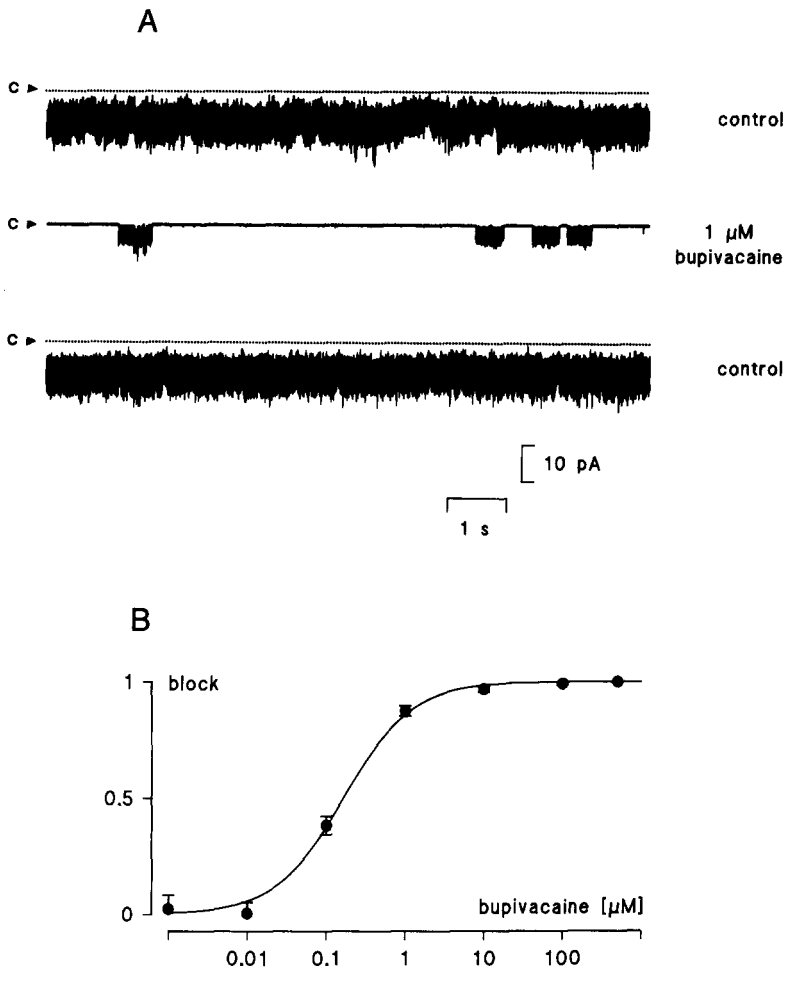

Fig. 10. Bupivacaine block. (*A*) Recordings with 105 mM-K_o (control), with 105 mM-K_o containing 1 μM bupivacaine in the bath and wash out, outside-out patch, pipette: 105 mM-K_i, E_m = −100 mV. Three channels were open at most times in the control recordings. (*B*) Fractional block of total mean current *vs.* concentration of bupivacaine at the same potential. Data from six outside-out patches. The curve was obtained as in Fig. 7*B* with IC_{50} = 0.165 μM and a = 1.0.

potential of the flicker channel (−70 mV) nearly matches the resting potential of myelinated nerve fibers under physiological conditions (−71 mV, Huxley & Stämpfli, 1951; −60 to −80 mV, Barrett & Barrett, 1982). Moreover, the classical observation that 5 mM TEA depolarizes myelinated nerve fibers by only 3 to 4 mV (Schmidt & Stämpfli, 1966) suggests that the channels setting the resting potential are weakly TEA-sensitive. From the "macropatch" measurements we conclude that a substantial part of the specific membrane conductance at the resting potential in myelinated axons is caused by the flicker channel. The flicker channel has been observed in nodal, paranodal, and internodal regions of the axonal membrane of the thin myelinated nerve fiber in high density. It has been demonstrated that paranodal and internodal K channels contribute to the resting potential (Chiu & Ritchie, 1984), and therefore it is likely that not only the nodal but also the para- and internodal flicker channels contribute to the resting potential of the myelinated nerve fiber. In order to elucidate the contribution of the flicker channel to the resting potential under physiological conditions, pharmacological investigations similar to the experiments described here have to be carried out on the intact nerve fiber or even on the whole nerve in vivo. For such experiments, the detailed pharmacological profile established in the present paper is essential.

However, it already seems clear that in different cell types the resting potential is determined by different K channels. In muscle, it is mainly determined by a K-selective inward rectifier (Adrian, Chandler & Hodgkin, 1970). In the β-cell, ATP-sensitive K channels (Ashcroft, Ashcroft & Harrison, 1988) mainly determine the resting potential, in *Aplysia* sensory neurons, the K-selective outwardly rectifying S current (Klein, Camardo & Kandel, 1982), and in thin myelinated nerve the flicker channel may play a role. Thus, it seems that evolution has developed

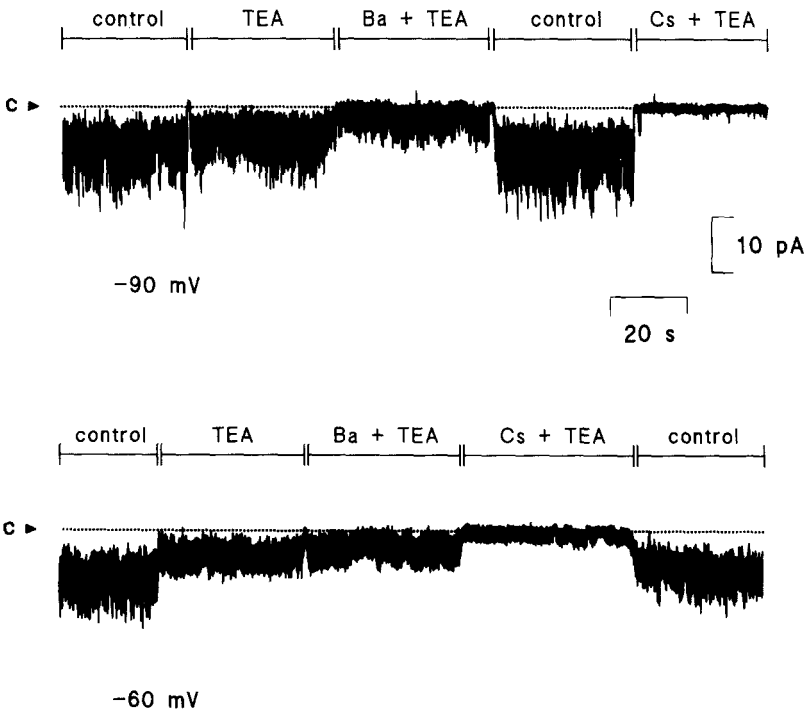

Fig. 11. Pharmacological blockade of holding currents at $E_m = -90$ mV (upper trace) and $E_m = -60$ mV (lower trace). Holding currents from an outside-out macropatch with 105 mM-K_i in the pipette were recorded in different external solutions: 105 mM-K_o (control), 10 mM TEA + 105 mM-K_o (TEA), 1 mM Ba + 10 mM TEA + 105 mM-K_o (Ba + TEA), and 10 mM Cs + 10 mM TEA + 105 mM-K_o (Cs + TEA). Record at −60 mV was obtained >1 min after the voltage step to this potential when the current was stationary. Pipette resistance: 18 MΩ.

various principles for generating the resting potential in distinct cell types.

A grant from the Konrad-Adenauer-Stiftung to D.-S.K. is gratefully acknowledged, and this paper constitutes a part of his dissertation. We thank Drs. H. Bostock, B. Neumcke, D. Siemen and Mr. G. Reid for reading the manuscript and Mrs. Elke Schmidt for technical assistance. Financial support was received from the Deutsche Forschungsgemeinschaft (Vo188/13-2).

References

Adrian, R.H., Chandler, W.K., Hodgkin, A.L. 1970. Slow changes in potassium permeability in skeletal muscle. *J. Physiol.* **208:**645–668

Ashcroft, F.M., Ashcroft, S.J.H., Harrison, D.E. 1988. Properties of single potassium channels modulated by glucose in rat pancreatic β-cells. *J. Physiol.* **400:**501–527

Baker, M., Bostock, H., Grafe, P., Martius, P. 1987. Function and distribution of three types of rectifying channel in rat spinal root myelinated axons. *J. Physiol.* **383:**45–67

Barrett, E.F., Barrett, J.N. 1982. Intracellular recording from vertebrate myelinated axons: Mechanism of the depolarizing afterpotential. *J. Physiol.* **323:**117–144

Chang, D.C. 1986. Is the K permeability of the resting membrane controlled by the excitable K channel? *Biophys. J.* **50:**1095–1100

Chiu, S.Y., Ritchie, J.M. 1982. Evidence for the presence of potassium channels in the internode of frog myelinated nerve fibres. *J. Physiol.* **322:**485–501

Chiu, S.Y., Ritchie, J.M. 1984. On the physiological role of internodal potassium channels and the security of conduction in myelinated nerve fibres. *Proc. R. Soc. Lond.* **B220:**415–422

Colquhoun, D., Hawkes, A.G. 1982. On the stochastic properties of bursts of single ion channel openings and of clusters of bursts. *Philos. Trans. R. Soc. London* **B300:**1–59

Colquhoun, D., Sigworth, F.J. 1983. Fitting and statistical analysis of single-channel records. *In:* Single-Channel Recording. B. Sakmann and E. Neher, editors. pp. 191–263. Plenum, New York and London

Constanti, A., Galvan, M. 1983. Fast inward-rectifying current accounts for anomalous rectification in olfactory cortex neurones. *J. Physiol.* **385:**153–178

DeFelice, L.J. 1981. Introduction to Membrane Noise. Plenum, New York

Grygorezyk, R., Schwarz, W. 1985. Ca^{2+}-activated K^+ permeability in human erythrocytes: Modulation of single-channel events. *Eur. Biophys. J.* **12:**57–65

Hagiwara, S., Miyazaki, S., Rosenthal, N.P. 1976. Potassium current and the effect of cesium on this current during anomalous rectification of the egg cell membrane of a starfish. *J. Gen. Physiol.* **67:**621–638

Halliwell, J.V., Adams, P.R. 1982. Voltage-clamp analysis of muscarinic excitation in hippocampal neurons. *Brain Res.* **250:**71–92

Hamill, O.P., Marty, A., Neher, E., Sakmann, B., Sigworth, F.J. 1981. Improved patch-clamp techniques for high-resolution current recording from cells and cell-free membrane patches. *Pfluegers Arch.* **391:**85–100

Hamill, O.P. 1983. Potassium and chloride channels in red blood cells. *In:* Single-Channel Recording. B. Sakmann and E. Neher, editors. pp. 451–471. Plenum, London

Haydon, D.A., Requena, J., Simon, A.J.B. 1988. The potassium conductance of the resting squid axon and its blockage by clinical concentrations of general anaesthetics. *J. Physiol.* **402:**363–374

Hille, B. 1973. Potassium channels in myelinated nerve: Selective permeability to small cations. *J. Gen. Physiol.* **61:**669–686

Hille, B. 1992. Ionic Channels of Excitable Membranes. Sinauer, Sunderland

Hille, B., Schwarz, W. 1978. Potassium channels as multi-ion single-file pores. *J. Gen. Physiol.* **72:**409–442

Huxley, A.F., Stämpfli, R. 1951. Direct determination of membrane resting potential and action potential in single myelinated nerve fibres. *J. Physiol.* **112:**476–495

Hwa, G.G.C., Avoli, M. 1991. Hyperpolarizing inward rectification in rat neocortical neurons located in the superficial layers. *Neurosci. Lett.* **124:**65–68

Jack, J.J.B. 1976. Electrophysiological properties of peripheral nerve. *In:* The Peripheral Nerve. D.N. Landon, editor. pp. 740–818. Chapman and Hall, London

Jonas, P., Bräu, M.E., Hermsteiner, M., Vogel, W. 1989. Single-channel recording in myelinated nerve fibers reveals one type of Na channel but different K channels. *Proc. Natl. Acad. Sci. USA* **86:**7238–7242

Jonas, P., Koh, D.-S., Kampe, K., Hermsteiner, M., Vogel, W. 1991. ATP-sensitive and Ca-activated K channels in vertebrate axons: novel links between metabolism and excitability. *Pfluegers Arch.* **418:**68–73

Jones, S.W. 1989. On the resting potential of isolated frog sympathetic neurons. *Neuron* **3:**153–161

Klein, M., Camardo, J., Kandel, E.R. 1982. Serotonin modulates a specific potassium current in the sensory neurons that show presynaptic facilitation in *Aplysia*. *Proc. Natl. Acad. Sci. USA* **79:**5713–5717

Koh, D.-S., Jonas, P., Bräu, M., Hermsteiner, M., Vogel, W. 1991. A TEA-insensitive potassium channel with complex gating recorded from amphibian myelinated nerve fibres. *Pfluegers Arch.* **418:**R30

Mayer, M.L., Westbrook, G.L. 1983. A voltage-clamp analysis of inward (anomalous) rectification in mouse spinal sensory ganglion neurones. *J. Physiol.* **340:**19–45

McManus, O.B., Magleby, K.L. 1988. Kinetic states and modes of single large-conductance calcium-activated potassium channels in cultured rat skeletal muscle. *J. Physiol.* **402:**79–120

Nonner, W. 1969. A new voltage clamp method for Ranvier nodes. *Pfluegers Arch.* **309:**176–192

Quayle, J.M., Standen, N.B., Stanfield, P.R. 1988. The voltage-dependent block of ATP-sensitive potassium channels of frog skeletal muscle by caesium and barium ions. *J. Physiol.* **405:**677–697

Rae, J.L., Dewey, J., Cooper, K. 1989. Properties of single potassium-selective ionic channels from the apical membrane of rabbit corneal endothelium. *Exp. Eye Res.* **49:**591–609

Sakmann, B., Neher, E. 1983. Geometric parameters of pipettes and membrane patches. *In:* Single-Channel Recording. B. Sakmann, and E. Neher, editors. pp. 37–51. Plenum, New York and London

Sakmann, B., Trube, G. 1984. Voltage-dependent inactivation of inward-rectifying single-channel currents in the guinea-pig heart cell membrane. *J. Physiol.* **347:**659–683

Schmidt, H., Stämpfli, R. 1966. Die Wirkung von Tetraäthylammoniumchlorid auf den einzelnen Ranvierschen Schnürring. *Pfluegers Arch.* **287:**311–325

Spalding, B.C., Swift, J.G., Horowicz, P. 1986. Zinc inhibition of potassium efflux in depolarized frog muscle and its modification by external hydrogen ions and diethylpyrocarbonate treatment. *J. Membrane Biol.* **93:**157–164

Takahashi, T. 1990. Inward rectification in neonatal rat spinal motoneurones. *J. Physiol.* **423:**47–62

Yamamoto, D., Suzuki, N. 1987. Blockage of chloride channels by HEPES buffer. *Proc. R. Soc. London* **B230:**93–100

Yellen, G. 1984. Ionic permeation and blockade in Ca^{2+}-activated K^+ channels of bovine chromaffin cells. *J. Gen. Physiol.* **84:**157–186

Received 2 January 1992; revised 20 May 1992